Computer Communications 34 (2011) 1883–1891

Contents lists available at ScienceDirect

Computer Communications

journal homepage: www.elsevier.com/locate/comcom

Analytical modelling in 802.11 ad hoc networks

Kinda Khawam [a,*], Marc Ibrahim [a], Marwen Abdennebi [b], Dana Marinca [a], Samir Tohme [a]

[a] Universite de Versailles, Saint Quentin en Yvelines, France
[b] Ecole Superieure des Ingenieurs de Beyrouth Mar Roukos – Mkallès B.P. 1514 – Riad El Solh, 1107 2050 Lebanon

ARTICLE INFO

Article history:
Received 22 June 2010
Received in revised form 20 January 2011
Accepted 15 May 2011
Available online 23 May 2011

Keywords:
Analytical modelling
802.11 ad hoc networking
The MAC protocol
Interference
Fading

ABSTRACT

This paper tries to bring together the physical model and protocol model that have been used to characterize interference relationship in an 802.11 ad hoc network. The physical model (known as the SNR model) is generally considered as a reference model for the physical layer behaviour but its application in wireless ad hoc networks is restricted by its complication. On the other hand, the protocol model (known as the unified disk graph) is straightforward but its validity is doubtful. We propose an analytical model for 802.11 ad hoc wireless networks where both the physical and protocol models are improved and modelled accurately by taking into accounts all emitters in the network and circumventing simplistic assumptions where communications are supposed to systematically fail if non-intended emitters fall in proximity of a receiver node. Our model consists in replacing a finite number of nodes by an equivalent continuum – characterized by a density of nodes – and disseminated in the network according to some distribution function. The key feature of the proposed model is that it permits taking into account the effect of interference, the CSMA/CA mechanism and radio propagation aspects in an easy and clear-cut way. All assumptions in the model are assessed with simulation results. Closed form formula of the signal to noise ratio and the throughput capacity per node will be given, corroborated by extensive simulation results in ns-2.

1. Introduction

Ad hoc networks are considered as a key factor in the evolution of wireless communication. The reason behind their augmented importance is twofold: first, with the increase of small size information processing devices, the need to exchange digital information is ever increasing. Second, ad hoc networking has been proven to be a promising solution to increase radio coverage of broadband wireless systems. In fact, ad hoc networks will be interconnected to telecom operator networks to enhance the access granularity. However, the lack of any wired infrastructure, the nature of the wireless channel, and the need for robustness and scalability create many design problems [1,2] and render the modelling task of wireless ad hoc networks both crucial and challenging.

Given the low cost of ad hoc technology, it was suggested to use an over dimensioning planning approach based on a high density of nodes. Unfortunately, this should be done with care as increasing the density of nodes may have a negative impact on the capacity achieved per node [3]. Indeed, ad hoc network capacity is constrained by mutual interferences of concurrent transmissions between nodes. As long as all nodes use the same frequency band for communication, any node-to-node transmission will add to the level of interference experienced by other nodes. Therefore, for performance evaluation of mobile wireless ad hoc networks, it is vital to take into account the impact of interference.

1.1. Related work

There has been significant interest in ad hoc networks but not enough work has been carried out on the analytic modelling of their capacity from radio interference point of view. Theoretical capacity bounds on ad hoc network capacity are derived in [4] based on asymptotic analysis. Nonetheless, these results do not reveal the exact capacity of a network with a given number of nodes. In [5,6], a model for calculation of interference levels in wireless ad hoc networks is proposed. However, the proposed model uses a regular lattice for possible locations of mobile nodes (which is contradictory with the complete freedom of nodes' movement in ad hoc networking). In [7], the capacity of an ad hoc network is evaluated without resorting to a regular lattice model. In [8], authors extend the model of Bianchi [27] and proposes a model where nodes can interfere with others without being in their vicinity (the hidden node problem). In [9], delay and throughput performances are analyzed under Poisson traffic while considering the hidden nodes in the network. The paper in [10] develops an analytical model that resorts to simple heuristics and approximations of collision and backoff times caused by

* Corresponding author. Tel.: +33 675653901.
E-mail address: kindakhawam@hotmail.com (K. Khawam).

0140-3664/$ - see front matter © 2011 Elsevier B.V. All rights reserved.
doi:10.1016/j.comcom.2011.05.008

interference from non-neighbouring nodes, however not from all active nodes in the network. Furthermore, the vast majority of analytical modelling effort was made under ideal channel conditions. As far as imperfect channel conditions is concerned, the authors in [11,12] have investigated the impact of capture on the capacity of the IEEE 802.11 in both Rayleigh- and Rician-fading channels. However, no provision was made to consider the interdependencies among the nodes. In [13], a thorough model is proposed where the impact of the physical layer, the MAC layer and the topology are taken into account. The models proposed are different from those present in this paper (in particular, a linear topology is presented and the fading impact is assessed through simulations). Lately, the CSMA mechanism was modelled analytically in [14–16]. In [14], the paper considers only pairwise interference and carrier-sensing decision models whereas in [15], an improved interference model is proposed but fails however to consider all nodes in the network. In [16], an ideal CSMA network is modelled as a set of interacting on–off telegraph processes.

In most existing publications, there are two broadly used models to characterize interference interactions in a wireless network, which are the physical model and the protocol model. The physical model is based on practical transmitter designs of communication systems that treat interference as noise. Under the physical model, a transmission is successful if and only if signal-to-noise-ratio (SNR) at the receiver node exceeds a threshold so that the transmitted signal can be decoded with an acceptable bit error probability. Still, the intricacy related with the physical model is the difficulty in obtaining a tractable solution, particularly in a network environment with concurrent communications. To evade the complexity issue associated with physical model, the so-called protocol model in [4], also known as unified disk graph model, has been widely used in the literature to simplify the analytical characterization of physical layer. Under the protocol model, a successful transmission occurs when a node falls inside the transmission range of its intended emitting node and falls outside the interference ranges of other non-intended emitting nodes. The setting of transmission range is based on a signal-to-noise-ratio (SNR) threshold. Under the protocol model, the impact of interference from a transmitting node is binary and is exclusively determined by whether or not a receiver falls within the interference range of its transmitting node. That is, if a node falls in the interference range of non-intended transmitting nodes, then this node is considered to be intensively interfered and thus communication fails. Otherwise, the interference is assumed to be insignificant. Due to such simplification, the protocol model has been broadly used in developing algorithms and protocols in wireless ad hoc networks (e.g. [18]) and can be easily used to analyze large wireless networks. The paper in [26] shows in what authors call 'reality check' that this model is too simplistic as it fails to give accurate results in realistic settings.

1.2. Paper contribution

The principal argument against the protocol model is that a binary decision of whether or not interference exists (based on interference range) does not precisely capture physical layer characteristics. For the case when a node falls in the interference range of non-intended emitting nodes, the protocol model assumes that the communication fails (due to interference). But this is overly conservative as there could still be some capacity even with interference. On the other hand, for the case when a node falls outside the interference range of each non-intended transmitting node, protocol model assumes that there is no interference. But this is too optimistic as small interference from different transmitters can aggregate and become non negligible. The goal of this paper is to reconcile the strain between the physical model and the protocol model. On the one hand, we propose a different protocol model that takes into account the fading of the physical channel. On the other hand, we put forward a physical model where the impact of all transmitting nodes in the network is accounted for. Hence, for the case when a node falls in the interference range of a non-intended transmitter node, the transmission can succeed if the SNR at the receiver is greater than a minimal threshold. To evaluate analytically the impact of interference while taking into account the effect of fading and the interactions between the physical and the protocol models, we propose an analytical model for the saturated, per-node, single-hop capacity for an 802.11b ad hoc network. In the proposed model, a finite number of nodes is replaced by an equivalent continuum to ease mixing the effects of interference, the cogwheel of the CSMA/CA protocol and the variability of the radio resource due to fading, as well as the interaction between the physical and protocol models. We only assume that nodes are uniformly distributed in the network which is fairly plausible in unmanaged community networks. Part of this work was already published in [3], however the analytical model was not exhaustive as it relied solely on the Bianchi model in [27] which is not appropriate in a real network setting. Furthermore, all results are here validated through extensive simulations in ns-2 which was overlooked previously due to the task complexity and lack of time. More importantly, parts of the model that did not succeed to match simulation results were either corrected or dropped.

1.3. Paper organization

The rest of the paper is organized as follows. In Section 2, we describe the protocol model by presenting assumptions used for the radio channel and illustrating accordingly our fluid analytical model to assess the impact of interfering nodes. In Section 3, the physical model is put forward by computing the SNR perceived by receiving nodes. The expression of the SNR is put to contribution to compute the mean feasible rate. The interaction between the protocol and physical models is presented in Section 4 to lead to an accurate computation of the throughput capacity per node in Section 5. In Section 6, we prove the exactness of our analytical model through extensive ns-2 simulations. We conclude in Section 7.

2. The protocol model

In this section, we depict the protocol model by first portraying the models for the radio resource, the location of nodes and the CSMA/CA mechanism. The presented analytical model replaces a finite number of nodes by an equivalent continuum characterized by a density of nodes ρ. We define an area around the transmitting node, termed contention domain, where all communications must seize according to the CSMA/CA mechanism in order to fulfil the necessary condition for a successful transmission. Accordingly, we compute the density of transmitting nodes outside the contention domain in order to take into account all interfering nodes in the network. Hence, contrary to the usual protocol model, if a node falls in the interference range of non-intended transmitting nodes, then the latter node is not considered to be intensively interfered so that it cannot receive correctly from its intended transmitter.

2.1. The density of nodes

Our model assumes a uniform distribution of nodes of density ρ_n over a two-dimensional area of limited size (the network surface is a disc of ray R_{Net}). If n is the total number of nodes present in the network, ρ_n is given by the following:

$$\rho_n = \frac{n}{\pi \cdot R_{Net}^2} \quad (1)$$

2.2. The radio channel

To obtain an accurate model for the radio channel, both path loss and fading are considered. The power received by a given node k depends on the radio channel state and varies with time due to fading effects.

Let P be the transmission power of a transmitting node k^*, γ_k the free space path loss and X_k the fast fading effect experienced by node k.

The power received by a node k situated at a distance r_k from the transmitting node, at time t, is then given by:

$$P_k(r_k, t) = P \cdot \gamma_k(r_k) \cdot X_k(t) \quad (2)$$

We do not consider power control and thus we assume that all nodes have the same transmitting power. As for fading, the random variables X_k are i.i.d. and follow an exponential distribution of parameter λ as we consider Rayleigh fading [29]. As we assume stationarity, the time index will be omitted in what follows.

The adopted model for the path loss is:

$$\gamma_k(r_k) = A \cdot \left(\frac{1}{r_k}\right)^{\beta}$$

with β being the path loss exponent varying between 2 and 5 and $A = (r_{min})^{\beta}$ where r_{min} is the minimal distance below which there is no power loss.

2.3. The contention domain

The receiving node k is said to be covered by the transmitting node k^* if the received power P_k is greater than some detection threshold P_{Th}. We define a geographical region around the transmitting node where nodes are covered with at least probability α:

$$\mathbb{P}(P_k > P_{Th}) \geqslant \alpha \Rightarrow \mathbb{P}\left(X_k > \frac{P_{Th}}{A \cdot P} \cdot r_k^{\beta}\right) \geqslant \alpha \Rightarrow e^{-\lambda \frac{P_{Th}}{A \cdot P} r_k^{\beta}} \geqslant \alpha$$

$$\Rightarrow r_k \leqslant R = \left(\ln\left(\frac{1}{\alpha}\right) \cdot \frac{A \cdot P}{P_{Th} \cdot \lambda}\right)^{1/\beta} \quad (3)$$

For a high value of α, this region – which is a disc of ray R centred on the transmitting node (as shown in Fig. 1)-approximates the contention domain (denoted by CD) of the transmitting node.

2.4. The density of transmitting nodes

The density of successfully transmitting nodes is evaluated in this section. In other words, the density of interferers is pinpointed as the set of successful transmitters generating interference for a given active connection. The basic WLAN MAC method for controlling the medium access is based on the CSMA/CA contention principle [28]. Using CSMA/CA, a node with a packet to transmit senses the channel to avoid collisions with on-going transmissions. If the channel is sensed idle, the node transmits. Otherwise, the node generates a random backoff interval before transmitting to minimize the probability of collision with any on-going transmission. Note that the RTS/CTS mechanism is not used.

Roughly speaking, two nodes can successfully transmit at the same time if they do not belong to the CD of each other as shown in Fig. 2. In Fig. 3, we portray the configuration of the maximum number of simultaneously successful transmitting nodes. In that extreme situation, the closest that a transmitting node can be situated from another transmitting (interfering) node is at the CD edge of the latter. Hence, there will be no more then one successful transmitter per a surface of radius $R/2$. Thus the maximum density of simultaneously successful transmitting nodes is:

$$\rho^* = \frac{4}{\pi \cdot R^2} \quad (4)$$

Simulations were run to assess the analytical model for the maximum density of successfully transmitting nodes ρ^*. Results are depicted in Fig. 4: the density of simultaneously transmitting nodes are plotted as a function of nodes density and compared to the constant theoretical value in (4) (constant for a given set of parameters). We see that simulation results tend to the value in (4) for large enough nodes densities. For low densities, the network is too poorly populated to match the theoretical result.

In Fig. 5, ρ^* is graphed for one simulation run as a function of time. We see that the density of transmitters increases to attain a constant value in the stationary regime, a value which is around the theoretical result.

3. The physical model

In this section, the physical model is presented through the SNR computation perceived at a given receiver. Owing to the fluid analytical model proposed, the impact of all interfering nodes outside the transmitter CD are taken into account. Accordingly, the probability that the SNR is greater than a given threshold is obtained. Finally, the latter result is used to derive the mean feasible rate of a receiving node as modulation and coding constraints in the 802.11 standards dictate its value.

3.1. The signal-to-noise ratio

The signal-to-noise ratio of a receiving node k, termed SNR_k, belonging to the CD of a transmitting node k^* is equal to:

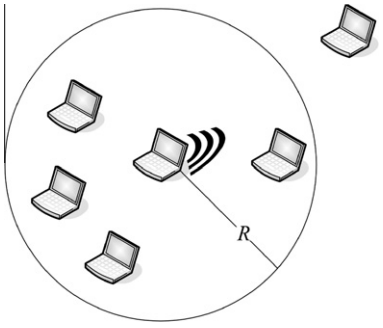

Fig. 1. Contention domain of a transmitting node.

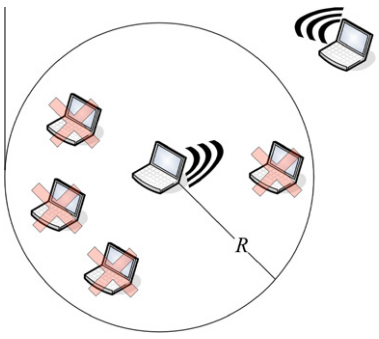

Fig. 2. ONE transmitting node in every CD.

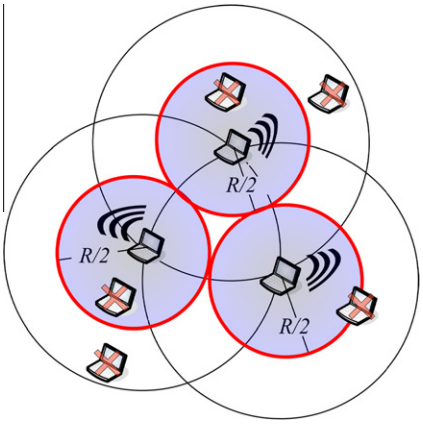

Fig. 3. Maximum density of transmitting node.

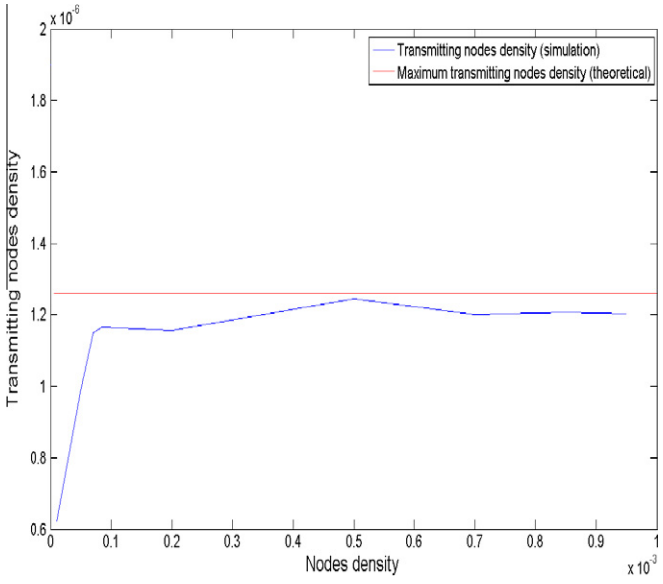

Fig. 4. ρ^* as a function of ρ_n (in km^{-2}).

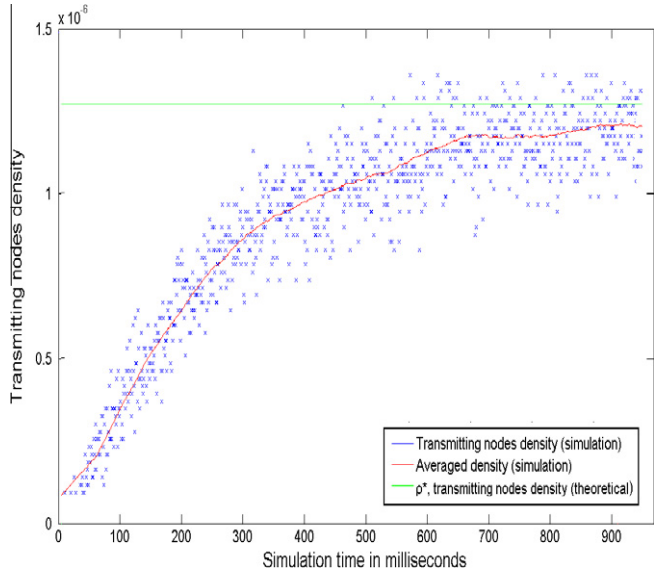

Fig. 5. The convergence of ρ^* (in km^{-2}).

$$SNR_k = \frac{P_k}{(\eta + I_k)} \tag{5}$$

where η is the background noise defined as a function of transmitting power $\eta = \epsilon \cdot P$ and I_k is the interference endured by node k and generated by other transmitting nodes (outside the *CD* of node k^*) and given by:

$$I_k = \sum_{i^*} P \cdot \gamma_{i^*,k} \cdot X_{i^*} = P \cdot \sum_{i^*} \frac{A \cdot X_{i^*}}{(r_{i^*,k})^\beta} \tag{6}$$

with $r_{i^*,k}$ being the distance between node k and each transmitting node i^* (except node k^*).

To obtain the radio signal with a given quality, the *SNR* needs to be greater than a given threshold. Therefore, we compute the probability that the SNR_k of node k exceeds a threshold δ_j, denoted by $S_{k,j}$ and given by $S_{k,j} = \mathbb{P}(SNR_k \geqslant \delta_j)$.

The following proposition renders the expression of $S_{k,j}$ while the proof substantiating it is given in the appendix.

Proposition 1. *The $S_{k,j}$ value is approximated by the following:*

$$S_{k,j} \approx e^{-\frac{\lambda \delta_j \eta r_k^\beta}{A \cdot P}} \cdot e^{-\delta_j \cdot r_k^\beta \cdot \theta} \tag{7}$$

where $\theta = \sum_{i^*} \left(\frac{1}{r_{i^*,k}}\right)^\beta$.

To obtain a closed-form formula of $S_{k,j}$, we still need to compute the value of $\theta = \sum_{i^*} \left(\frac{1}{r_{i^*,k}}\right)^\beta$ in (7) that reflects the impact of interference.

To reach that goal, we first need to assume that the simultaneous transmitters are uniformly distributed in the cell. This assumption is validated by simulation results presented in the two sets of figures in 6 and 7. In Fig. 6, two random snapshots of the network are presented where only successful transmitters appear. We notice that they are fairly uniformly distributed in the network. Further, we considered a rectangular surface of $700 \times 700\ m^2$. The abscissa and ordinate of nodes are uniformly distributed relatively to the centre of the network space (in meter). In Fig. 7, we plot the position of nodes (in red the abscissa, in blue the ordinate) as well as the mean position obtained through simulation (the line in green in the figure) and compare these results to the theoretical value that appears in black. We notice that the mean value provided by simulation and that provided by the theoretical model are almost indistinguishable.

Proposition 2. *With the aid of the uniformity assumption, the value of θ is approximated as follows:*

$$\theta \approx 2\pi\rho^* R_{Net}^{-\beta+2} \left[\frac{[1 - \overline{R}^{2-\beta}]}{2-\beta} - d_k^2 \frac{\beta}{4}[1 - \overline{R}^{-\beta}] - d_k^4 \frac{\beta}{8}[1 - \overline{R}^{-\beta-2}] \right] \tag{8}$$

where $\overline{R} = \frac{R}{R_{Net}}$ and $d_k = \frac{r_k}{R_{Net}}$.

We compute the standard deviation between θ and its approximated value in (8) for $r_k \leqslant \frac{R}{4}$ realizing that the maximum deviation is approximately 5% at $r_k = \frac{R}{4}$ which is acceptable.

Finally, using (27) and (8), we get:

$$S_{k,j} = e^{-\delta_j \left\{ \frac{\lambda \eta r_k^\beta}{A \cdot P} + N d_k^\beta \left[\frac{[1-\overline{R}^{2-\beta}]}{2-\beta} - d_k^2 \frac{\beta}{4}[1-\overline{R}^{-\beta}] - d_k^4 \frac{\beta}{8}[1-\overline{R}^{-\beta-2}] \right] \right\}} \tag{9}$$

where $N = 2\pi R_{Net}^2 \rho^*$ is the total number of transmitting (interfering) nodes.

3.2. Instantaneous and mean rates

The value taken by the *SNR* determines the modulation scheme and therefore the instantaneous peak rate perceived by the serviced node. In practice, the set of achievable instantaneous peak

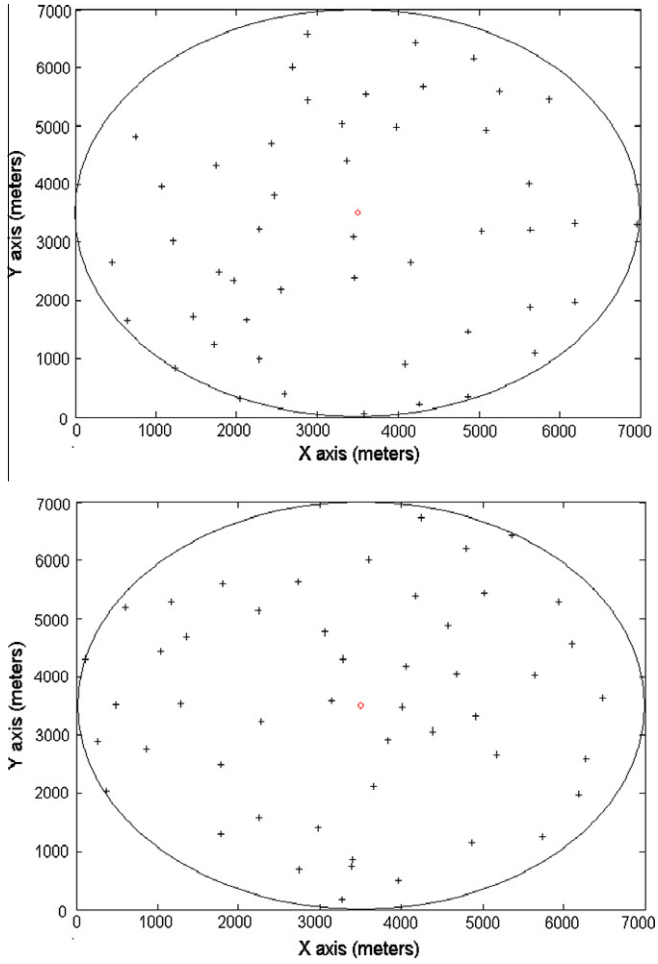

Fig. 6. Spatial distribution of transmitting nodes.

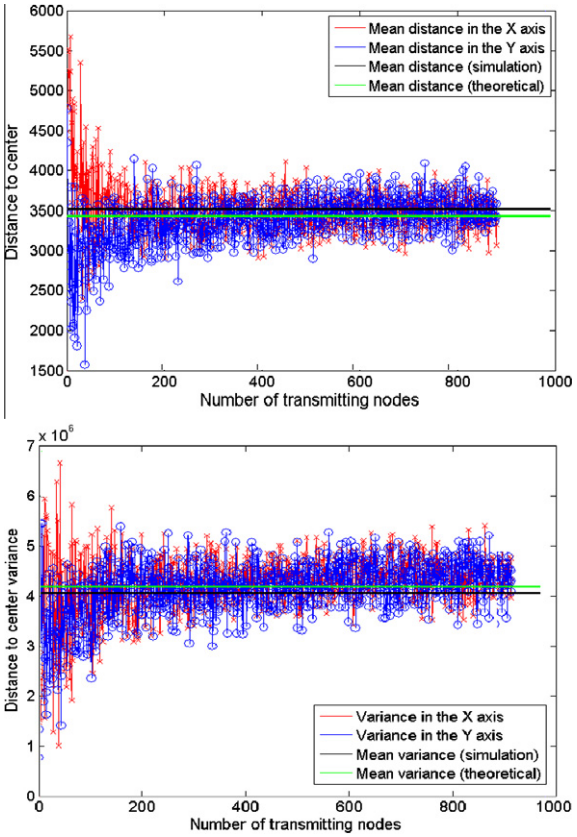

Fig. 7. Mean and variance of transmitting nodes position.

rates is not continuous. Indeed, coding constraints result in a discrete set of achievable rates $C_1 < C_2 < \cdots < C_M$.

The set of SNR thresholds δ_j for $0 \leqslant j < M$ and the corresponding discrete rates are obtained according to the 802.11b protocol [28] and are given in Table 1.

In particular, for correct reception of radio signals, the *SNR* needs to be equal or greater than a minimal threshold δ_0. In other words, a transmitting node cannot have direct communication with all nodes in its *CD* but only with those verifying the following inequality $SNR \geqslant \delta_0$.

Hence, the instantaneous rate $\Re_{r_k}$ of node k is given by:

$$\Re_{r_k} = \begin{cases} 0 & \text{if} SNR_k < \delta_0, \\ C_1 & \text{if} \delta_0 \leqslant SNR_k < \delta_1, \\ \dots & \\ C_M & \text{if} \delta_{M-1} \leqslant SNR_k. \end{cases} \tag{10}$$

Therefore, the mean feasible rate of node k, termed $\overline{\Re_{r_k}}$, and situated at distance r_k from the transmitter k^* is given by the following:

$$\overline{\Re_{r_k}} = \sum_{j=1}^{M} C_j \cdot \mathbb{P}(\delta_{j-1} \leqslant SNR_k < \delta_j) = \sum_{j=1}^{M} C_j \cdot (S_{kj-1} - S_{kj}) \tag{11}$$

with $\delta_M \equiv \infty$.

4. The interaction between physical and protocol models

Our analytical fluid model focuses on the essential aspects of the physical and protocol models, as well as their interaction. On the one hand, the protocol layer provides a scheduling discipline for nodes to access the shared channel of the network, and this discipline renders probabilities that nodes will attempt to transmit. On the other hand, the physical model encodes information attempting to ensure that the transmitted frames are received correctly which means that SNR ought to be greater than a minimal threshold; the likelihood with which a transmission is successful depends on how well the signaling used defends against channel impairments and interference from any source. Clearly, the dynamics of the protocol model is tightly connected to the dynamics of the physical model.

In the sequel, we build our modeling framework by expressing each model's functionality in probabilistic terms, i.e., in the physical model we are concerned with the probability of a successful frame transmission, whereas in the protocol model we are concerned with the collision probability.

Table 1
The set of discrete rates and SNR thresholds in 802.11b.

k	1	2	3	$M = 4$
C_j (Mbit/s)	1	2	5.5	11
δ_{j-1} (dB)	1	7	11	16

4.1. The successful reception probability

We denote by q_k the successful reception probability between transmitting node k^* and its receiver node k. The probability q_k depends on both the physical channel and the MAC mechanism as follows: for the protocol model, correct frame reception imposes that the SNR_k at node k is greater than the minimal threshold δ_0.

Concerning the protocol model, nodes around the receiver must hold their transmissions otherwise, correct reception is not guaranteed. This issue is commonly known as the hidden node problem. These particular interferers are situated in a *CD* around the receiver node k.

We suppose saturation at all nodes, i.e., all buffers are full. In this paper, we also assume that a packet is always available for transmission at the head of a node's queue. Thus, the successful reception probability is given by the following:

$$q_k = \mathbb{P}(SNR_k > \delta_0) \cdot \prod_{i \in CD_k} (1 - \tau_i) \tag{12}$$

where τ_{k^*} is the transmission probability of node k^* and $\mathbb{P}(SNR_k > \delta_0) = S_{k,0}$ according to formula (9).

The performance analysis of the CSMA/CA access scheme has been studied analytically by Bianchi in [27]. It is equivalent to solving a fixed point equation to determine the stationary transmission probability τ that a tagged node transmits in a randomly chosen time slot. However, in [27], all nodes belong to the same *CD* whereas in the present context we consider a realistic network scenario where different *CD*s coexist in the same network. The results in [27] are used for the interactions in the same *CD*, as for the impact of other *CD*s, it is accounted for through the value of the *SNR* at the receiving node that endures the effect of all simultaneous transmissions in the network.

In [13], the Bianchi model is generalized to a fully-connected network through a relation between τ_{k^*} and q_k:

$$\tau_{k^*} = \frac{2W_{min}}{(W_{min}+1)^2} \times q_k \tag{13}$$

where W_{min} is the minimal backoff window size of the MAC algorithm.

Assuming that $\frac{2W_{min}}{(W_{min}+1)^2} \ll 1$ and using the fact that $0 < q_k < 1$, formula (13) rewrites as:

$$q_k \approx S_{k,0} \cdot \left(1 - \sum_{i \in CD_k} \frac{2W_{min}}{(W_{min}+1)^2} q_i\right)$$

Summing over the number of nodes in a *CD*, we obtain what follows:

$$\sum_{k \in CD} q_k \approx \sum_{k \in CD} \left[S_{k,0} \cdot \left(1 - \sum_{i \in CD} \frac{2W_{min}}{(W_{min}+1)^2} q_i\right)\right] = \sum_{k \in CD} S_{k,0} - \frac{2W_{min}}{(W_{min}+1)^2} \sum_{k \in CD} S_{k,0} \cdot \sum_{i \in CD} q_i$$

Due to the uniformity of the network, all *CD*s are equivalent and perceive roughly the same conditions, hence we deduce the following result:

$$\sum_{k \in CD} q_k \approx \frac{\sum_{k \in CD} S_{k,0}}{1 + a \sum_{k \in CD} S_{k,0}} \tag{14}$$

where we define $a = \frac{2W_{min}}{(W_{min}+1)^2}$ for simplicity.

4.2. The Collision Probability

The probability ϕ_{k^*} of a collision seen by a transmitting node k^* is:

$$\phi_{k^*} = 1 - \prod_{i^* \in CD_{k^*}} (1 - \tau_{i^*}) \tag{15}$$

where CD_{k^*} is the *contention domain* of node k^*.

Resorting to the same assumptions used previously and using formula (14), the collision probability in (15) amounts to:

$$\phi_{k^*} \approx a \sum_{i^* \in CD_{k^*}} q_{i^*} = \frac{a \sum_{k \in CD} S_{k,0}}{1 + a \sum_{k \in CD} S_{k,0}} \tag{16}$$

Proposition 3. *Finally, according to our analytical model, formula (15) becomes:*

$$\phi \approx \frac{a \int_0^R S_{k,0}(r_k) \rho_n 2\pi r_k dr_k}{1 + a \int_0^R S_{k,0}(r_k) \rho_n 2\pi r_k dr_k} \tag{17}$$

Note that the collision probability owing to the uniformity assumption is now the same for all nodes in the network.

5. The throughput capacity

As mentioned earlier, the mean feasible rate $\overline{\Re_{r_k}}$ in (11) is obtained for a receiving node k situated at a distance r_k from the transmitter k^*. As a consequence, the expected value of the capacity in the *CD*, denoted by C_R, must be found by taking into account all possible positions of the receiver in the *CD* of a transmitting node. Therefore, with the assumption that the network nodes queues are always full and that all packets have the same size, we deduce the following:

$$C_R = \int_0^R (1 - \phi) \cdot \overline{\Re_{r_k}} dp_k \tag{18}$$

where $dp_k = \frac{2\pi r_k}{\pi R^2} dr_k$ is the probability that a node k is situated at a distance between r_k and $r_k + dr_k$ from the transmitter (uniform distribution of nodes).

We term by n_R the total number of nodes present in a *CD*. Thus, it is given by the following:

$$n_R = \int_0^R \rho_n \cdot 2\pi r dr = n \cdot \left(\frac{R}{R_{Net}}\right)^2 \tag{19}$$

In the basic form of CSMA/CA, the capacity in the *CD* is fairly shared among the n_R nodes. Using (11), (9) and (18), it follows that the throughput capacity per node, given by $\overline{C_R} = \frac{C_R}{n_R}$, amounts to the following:

$$\overline{C_R} = \frac{1 - \phi}{n} \cdot \left(\frac{R_{Net}}{R}\right)^2 \cdot \sum_{j=1}^{M} C_j \cdot [\xi_{j-1} - \xi_j] \tag{20}$$

where

$$\xi_j = \int_0^R \frac{2r_k dr_k}{R^2} \cdot e^{-\delta_j \left\{\frac{\lambda \eta r_k^\beta}{A P}\right\}} \cdot e^{-\delta_j \left\{N d_k^\beta \left[\frac{[1-\overline{R}^{2-\beta}]}{2-\beta} - d_k^{2\beta}[1-\overline{R}^{-\beta}] - d_k^{4\beta}[1-\overline{R}^{-\beta-2}]\right]\right\}}$$

6. Performance analysis

We present in this section some numerical results to illustrate the collision probability and the throughput capacity per node in order to answer basic planning questions. We consider the following parameters in Table 2 which are fairly realistic and are chosen to give insight on the network performances. Nodes were scattered uniformly in the simulation space.

The set of SNR thresholds and the corresponding discrete rates are already given in Table (1). Simulations were run in well-known Network Simulator ns-2 [30]. To measure the real effect of the SNR on capacity, we changed the 802.11 physical layer in ns-2 simulator, based on the extended MAC/PHY module provided by [31]. Furthermore, this module has an enhanced computation model for the SNR and various modulations schemes. We improved this part by adding the automatic rate adaptation through the adaptation of the modulation scheme to the measured SNR at the receiver node.

To validate formula (3) that gives the *CD* radius termed R, we computed the relative deviation between the theoretical value of R (by applying the above simulation parameters in (3) for a cover-

Table 2
Simulations parameters.

β	3.0 (urban environment)
ϵ	10^{-10}
A	3.375 (maximal power at $r_{min} = 1.5$ m)
Maximal power P	100 mW
Threshold power P_{th}	$3 \cdot 10^{-7}$ mW
λ	1 (fading of unit mean)
MAC minimal backoff window size W_{min}	32
MAC maximal backoff window size W_{max}	1024
R_{Net}	2500 m

age probability of $\alpha = 0.9$) and the numerical value of R obtained via simulation. The result is around 0.047.

6.1. Collision probability

The collision probability ϕ is depicted in Fig. 8 as a function of nodes density ρ_n. In the upper figure, simulation results are presented while in the lower figure, ϕ is obtained according to the analytical model in (17). Although, the two plotted curves have the same pattern, the values diverge as the analytical model overestimates the collision probability. For lower values of ρ_n, the two sets of values are pretty close; however, as ρ_n increases, collision augments rapidly in the theoretical model contrary to the simulation results. It seems that in the latter case, nodes are only impacted by other nodes in their direct neighbourhood: we can see in the upper graph that the collision probability hardly increases for large values of nodes density.

6.2. Throughput capacity

To assess our model, we depict the throughput capacity per node in Mbit/s as a function of r_k, the distance between every transmitting node and its corresponding receiving node. We present two scenarios: in Fig. 9 a non fading channel and in Fig. 10 a fast fading channel (Rayleigh model). We consider a nodes density of $\rho_n = 20/m^2$.

6.2.1. Non fading channel

As fading is here neglected, the random variables X_k vanish in Eqs. (2) and (6) and are replaced by 1. Hence, in view of (5), the inequalities in (10) define a set of concentric rings of external radius $r0 < r1 < \cdots < rM \leqslant R$ around the transmitting node, corresponding to regions where the achievable rates C_j, for $j \in [1,\ldots,M]$ are attained. In other words, receiving nodes located at a distance r_k ranging between $rj-1$ and rj from their transmitter get the peak rate C_{M-k}.

To obtain the numerical value of these radii, we solve the following equation:

$$SNR_k \leqslant \delta_j \quad \text{for } j \in [1,\ldots,M] \tag{21}$$

Theoretical values of theses radii appear in Fig. 9 in the abscissa axis as the toppling point from one achievable peak rate C_j to the other (numerical values of these rates appear also in Table 1). We see that the mean rates obtained by simulation vary closely around the theoretical achievable rate stages.

6.2.2. Fading channel

In a fading environment, we depict in Fig. 10 the throughput capacity per node $\overline{C_R}$ as given in (20). We can see that the different rates in the simulation and the corresponding mean rate are contiguous to the theoretical value graphed in green. We deduce that the proposed model for 802.11 ad hoc network describes faithfully performance in a real environment.

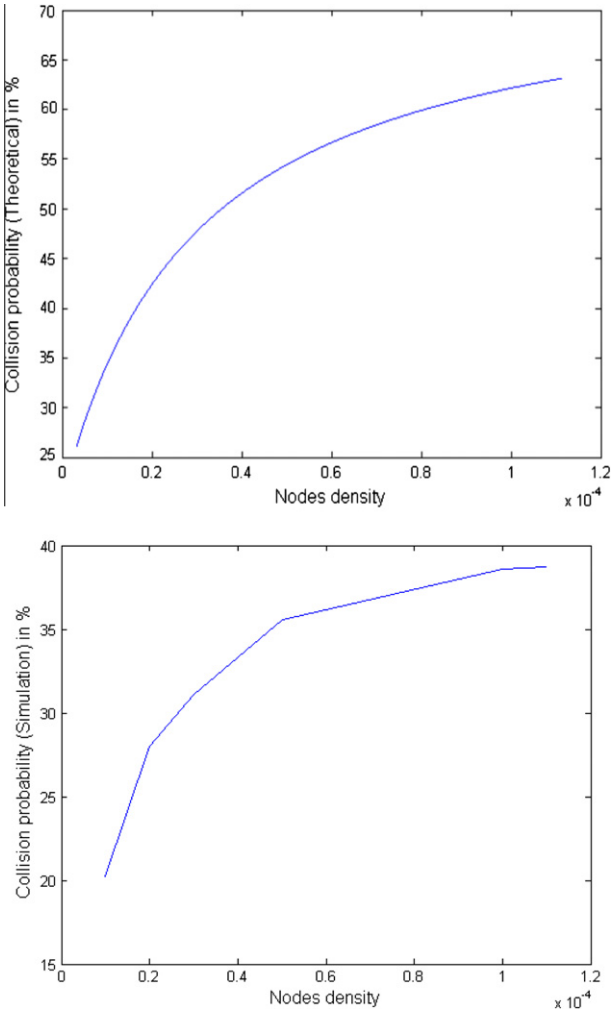

Fig. 8. Collision.

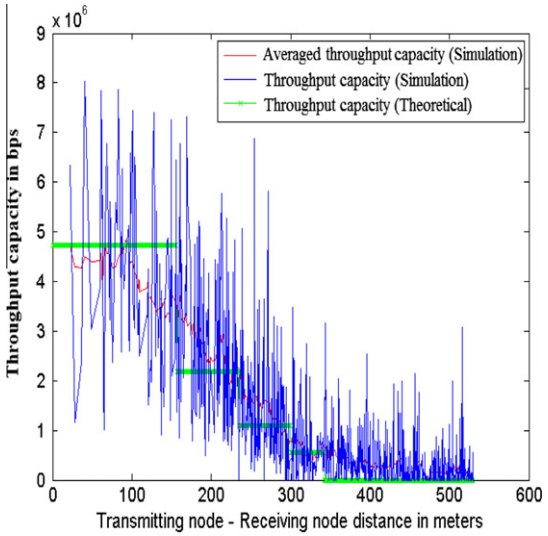

Fig. 9. Throughput capacity per node for a non fading channel.

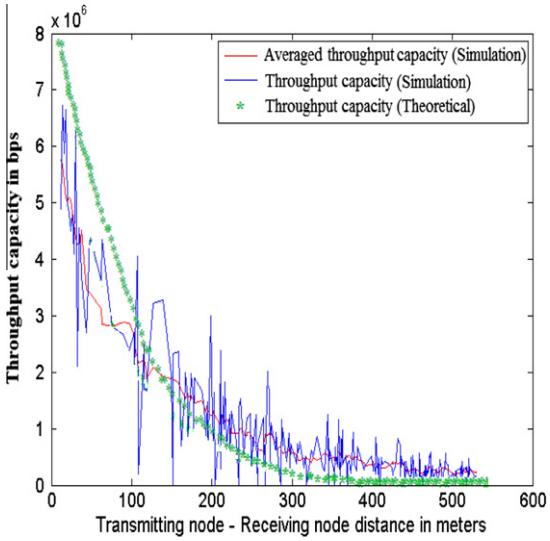

Fig. 10. Throughput capacity per node for a fading channel.

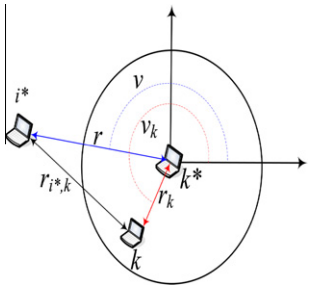

Fig. 11. Interference.

7. Conclusion

We have introduced a novel modelling framework for 802.11 ad hoc networks that explicitly takes into account the impact of the physical model and protocol model. The physical model is nearly exhaustive as it accounts for the path loss, the fading channel and the interference of all active nodes in the network. A key feature of our model is that a finite number of nodes is converted to an equivalent density of nodes making the model tractable without sacrificing its accuracy. The protocol model is improved and its interaction with the physical model is carefully considered. Our analytical model constitutes a tool for a fast, precise, and efficient evaluation of nodes performance for any configuration of a 802.11 ad hoc network, it is simple yet it does not sacrifice accuracy. The model provided closed form formulae for the throughput capacity and the collision probability of the CSMA/CA mechanism. Furthermore, analytical results were validated through discrete event simulations using the popular ns-2 tool, and the analytical results show a remarkable correlation with the results obtained via simulation. The importance of the analytical model is that the time needed to obtain the desired results takes a very small fraction of the time required to obtain the same results via discrete-event simulations. Finally, owing to the analytical model fluidity, it can easily be extended to evaluate performances in dense ad hoc networks [32].

Appendix A

A.1. Proof of proposition (1)

From the definition of $S_{k,j}$, we know that:

$$S_{k,j} = \mathbb{P}(X_k \geqslant \frac{\delta_j}{\gamma_k \cdot P} \cdot (I_k + \eta)) = \int_0^\infty \frac{\delta_j}{\gamma_k \cdot P} \cdot \lambda \cdot e^{-\lambda \cdot \frac{\delta_j}{\gamma_k P} u} \cdot \mathbb{P}(I_k + \eta \leqslant u) du \quad (22)$$

Knowing that the mean of a random variable X defined on a set $\varphi$is $\mathbb{E}[X] = \int_\varphi \mathbb{P}(X > u) du$, we deduce that:

$$\mathbb{E}[e^{-X}] = \int_\varphi e^{-u} \mathbb{P}(X \leqslant u) du \quad (23)$$

Using (22) and (23), and defining $\zeta_k = \frac{\lambda \cdot \delta_j}{\gamma_k \cdot P}$, we have that:

$$S_{k,j} = \mathbb{E}[e^{-\zeta_k \cdot (I_k + \eta)}] = e^{-\zeta_k \cdot \eta} \cdot \mathbb{E}[e^{-\zeta_k \cdot I_k}] \quad (24)$$

From (6) and (23), and defining $\zeta_{i^*,k} = \zeta_k \cdot P \cdot \gamma_{i^*,k}$, we deduce that:

$$\mathbb{E}[e^{-\zeta_k \cdot I_k}] = \prod_{i^*} \mathbb{E}[e^{-\zeta_k \cdot P \cdot \gamma_{i^*,k} \cdot X_{i^*}}] = \prod_{i^*} \zeta_{i^*,k} \int_0^\infty e^{-\zeta_{i^*,k} \cdot u} \cdot \mathbb{P}(X_{i^*} \leqslant u) du = \prod_{i^*} \frac{\lambda}{\lambda + \zeta_{i^*,k}} \quad (25)$$

We combine formulae (24) and (25) to obtain what follows:

$$S_{k,j} = e^{-\frac{\lambda \cdot \delta_j \cdot \eta}{\gamma_k P}} \cdot \prod_{i^*} \frac{1}{1 + \delta_j \frac{\gamma_{i^*,k}}{\gamma_k}} \quad (26)$$

To obtain a closed form formula for $S_{k,j}$, we approximate formula (26) as follows, due to the fact that $\delta_j \left(\frac{r_k}{r_{i^*,k}}\right)^\beta \ll 1$:

$$S_{k,j} = e^{-\frac{\lambda \delta_j \eta r_k^\beta}{A \cdot P}} \cdot \prod_{i^*} \frac{1}{1 + \delta_j \left(\frac{r_k}{r_{i^*,k}}\right)^\beta} \approx e^{-\frac{\lambda \delta_j \eta r_k^\beta}{A \cdot P}} \cdot e^{-\delta_j \sum_{i^*} \left(\frac{r_k}{r_{i^*,k}}\right)^\beta} \quad \square \quad (27)$$

A.2. Proof of proposition (2)

According to the plausible assumption of uniform distribution of transmitting nodes, we can write the following:

$$\theta = \int_0^{2\pi} \int_R^{R_{Net}} \left(\frac{1}{r_{i^*,k}}\right)^\beta \rho^* r dr dv \quad (28)$$

Using the generalized Pythagorean theorem that relates $r_{i^*,k}$ to r_k and r (see Fig. 11), we can re-write θ as follows:

$$\theta = \rho^* \int_0^{2\pi} \int_R^{R_{Net}} \frac{r^{-\beta+1}}{\left[1 + \frac{r_k}{r}\left(\frac{r_k}{r} - 2\cos(v - v_k)\right)\right]^{\frac{\beta}{2}}} dr dv \quad (29)$$

As $\frac{r_k}{r} < 1$, the denominator $\left[1 + \frac{r_k}{r}\left(\frac{r_k}{r} - 2\cos(v - v_k)\right)\right]^{\frac{\beta}{2}}$ in (29) is small enough to be well approximated with a taylor approximation at some low order. The smaller the ratio $\frac{r_k}{r}$, the lower the taylor order resulting in a simpler expression of $S_{k,j}$. As a consequence, we aim at determining more precisely the upper bound on $\frac{r_k}{r}$. We know that it is insufficient for a node to be present in the *CD* of a transmitter to communicate successfully with the latter: a receiving node k has to fulfil the following condition $\{SNR_k \geqslant \delta_0\}$. Hence, there is another geographical region, termed *Reception Domain RD*, around the transmitting node (smaller than the *CD*) where a node can receive the signal successfully. The *RD* is determined such as:

$$\mathbb{P}(SNR_k > \delta_0) \geqslant \alpha \Longleftrightarrow S_{k,0} \geqslant \alpha \quad (30)$$

We compute (30) numerically and deduce that, for $\frac{R}{R_{NET}} < 1$ and $2 \leqslant \beta \leqslant 6$, $\frac{r_k}{R} < \frac{1}{4}$ for $\alpha = 0.99$.

Thus, a tight approximation of θ is obtained at Taylor order 2:

$$\theta \approx \rho^* \int_0^{2\pi} \int_R^{R_{Net}} r^{-\beta+1} \left[1 - \frac{\beta}{2}\frac{r_k}{r}\left(\frac{r_k}{r} - 2\cos(v - v_k)\right) + \frac{\beta}{4}\left(\frac{\beta}{2} + 1\right)\frac{r_k^2}{r}\left(\frac{r_k}{r} - 2\cos(v - v_k)\right)^2\right.$$

A.3. Proof of proposition (3)

Using formula (13) and the approximation of $log(1+x)$ at Taylor order 1, we have the following:

$$\phi_{k^*} = 1 - \prod_{i^* \in CD_{k^*}} (1-\tau_{i^*}) = 1 - e^{\sum_{i^* \in CD_{k^*}} log(1-\tau_{i^*})} \approx 1 - e^{-\sum_{i^* \in CD_{k^*}} \tau_{i^*}}$$

$$\approx 1 - e^{-\sum_{i \in CD_{k^*}} \frac{2W_{min}}{(W_{min}+1)^2} q_i}$$

Furthermore, in view of formula (12) and making use of our analytical model, ϕ_{k^*} amounts to:

$$\phi_{k^*} \approx 1 - e^{-\frac{2W_{min}}{(W_{min}+1)^2} \int_0^R S_{i,0}(r_i)\rho_n 2\pi r_i dr_i} \quad (31)$$

We notice that ϕ_{k^*} is independent of the tagged node, hence the index $k*$ will be omitted after the integration in (15)). The reason behind this is our validated assumption concerning the spatial distribution of transmitters: as those nodes are uniformly distributed in the cell, a given communication is equally impacted by interferers, independently of the considered transmitter and emitter nodes. □

References

[1] IEEE J. Select. Areas Commun.: Special Issue Wireless Ad Hoc Netw., 17 (8) (1999).
[2] C.-K. Toh, Ad Hoc Mobile Wireless Networks: Protocols and Systems, first ed., Prentice Hall, Englewood Cliffs, NJ, 2001.
[3] K. Khawam, A.E. Samhat, M. Ibrahim, J.-M. Kelif, Fluid model for wireless adhoc networks, in: IEEE PIMRC, 2007.
[4] P. Gupta, P.R. Kumar, A. Viterbi, The capacity of wireless networks, IEEE Trans. Inform. Theor. (2000) 46.
[5] R. Hekmat, P. Van Mieghem, Interference in wireless multi-hop ad hoc networks and its effect on network capacity, Wireless Netw. 10 (2004).
[6] K. Bertet, C. Chaudet, I. Guerin Lassou, L. Viennot, Impact of Interferences on Bandwidth Reservation for Ad Hoc Networks: A First Theoretical Study, Globecom, 2001.
[7] P. Muhlethaler, A. Najid, Throughput Optimization in Multihop CSMA Mobile Ad Hoc Networks, European Wireless, 2004.
[8] Y. Barowski, S. Biaz, P. Agrawal, Towards the performance analysis of ieee 802.11 in multi-hop ad-hoc networks, in: WCNC 2005.
[9] Y. Chen, Q. Zeng, D. Agrawal, Analytical modeling of MAC protocol in ad hoc networks, Wireless Commun. Mobile Comput. 8 (2006).
[10] P. Siripongwutikorn, Throughput Analysis of an IEEE 802.1 lb Multihop ad hoc networks, in: IEEE/ACM Transactions on Networking, vol. 15, 2007.
[11] Z. Hadzi-Velkov, B. Spasenovski, The influence of at rayleigh fading channel with hidden terminals and capture over the IEEE802.11 WLANs, in: IEEE Vehicular Technology Conference, vol. 2, 2001.
[12] Z. Hadzi-Velkov, B. Spasenovski, On the capacity of IEEE 802.11 DCF with capture in multipath-faded channels, Int. J. Wireless Inform. Netw. 9 (2002).
[13] M. Carvalho, J.J. Garcia-Luna-Aceves, A scalable model for channel access protocols in multihop Ad Hoc networks, in: International Conference on Mobile Computing and Networking, 2004.
[14] L.B. Jiang, S.C. Liew, Improving throughput and fairness by reducing exposed and hidden nodes in 802.11 networks, IEEE Trans. Mobile Comput. 7 (2008).
[15] C. Chau, M. Chen, S. Liew, Capacity of Large-scale CSMA Wireless Networks, Mobicom, 2009.
[16] S.C. Liew, C. Kai, J. Leung, B. Wong, Back-of-the-envelope computation of throughput distributions in CSMA wireless networks, in: IEEE ICC, 2009.
[18] M. Alicherry, R. Bhatia, L. Li. Joint channel assignment and routing for throughput optimization in multi-radio wireless mesh networks, in: ACM Mobicom Proceedings, 2005, pp. 58–72.
[26] Y. Shi, Y. Thomas Hou, S. Kompella, How to correctly use the protocol interference model for multi-hop wireless networks, in Proceedings of ACM MobiHoc, 2009, pp. 239–248.
[27] G. Bianchi, Performance analysis of the IEEE 802.11 distributed coordination function, IEEE J. Selected Areas Commun. 18 (3) (2000).
[28] Wireless LAN Medium Access Control (MAC) and Physical Layer (PHY) specifications, ANSI/IEEE Std 802.11, 1999 Edition.
[29] B. Sklar, Rayleigh fading channels in mobile digital communication systems, IEEE Commun. Mag. 35 (7) (1997).
[30] Network Simulator, <http://nsnam.isi.edu/nsnam/index.php/User_Information>.
[31] Q. Chen, F. Schmidt-Eisenlohr, D. Jiang, M. Torrent-Moreno, L. Delgrossi, H. Hartenstein, Overhaul of IEEE 802.11 Modeling and Simulation in NS-2, in: The 10th ACM International Symposium on Modeling, Analysis and Simulation of Wireless and Mobile Systems, MSWIM, Greece, October 2007.
[32] P. Jacquet, Geometry of Information Propagation in Massively Dense Ad hoc Networks, in: The ACM International Symposium on Mobile Ad Hoc Networking and Computing, mobihoc 2004.